

## Low-Level Saturation of Brillouin Backscattering due to Cavity Formation in High-Intensity Laser-Plasma Interaction

S. Weber, C. Riconda, and V. T. Tikhonchuk

*Centre Lasers Intenses et Applications (CELIA), UMR 5107 CNRS–Université Bordeaux I–CEA, Université Bordeaux I, 33405 Talence, France*

(Received 26 March 2004; published 10 February 2005)

Full particle-in-cell simulations of Brillouin backscattering in the high-intensity regime are presented. The final state of the strongly nonlinear evolution of the ion-acoustic wave packet consists of its collapse and the formation of a density cavity which is supported by large-amplitude localized electromagnetic fields. The cavitation manifests itself in large oscillations of the reflectivity which is terminated by a low-level saturation with strong kinetic effects. This newly discovered scenario demonstrates the importance of fully kinetic descriptions of Brillouin backscattering for high intensities.

DOI: 10.1103/PhysRevLett.94.055005

PACS numbers: 52.35.Mw, 52.38.Bv, 52.38.Kd, 52.65.Rr

Stimulated Brillouin backscattering (SBBS) is a three-wave interaction process where an electromagnetic wave incident on a plasma of density less than the critical one decays into a backscattered electromagnetic wave of almost the same frequency and a forward propagating ion-acoustic wave (IAW). The backscattered wave represents a loss of energy otherwise available for interaction. The observed levels of backscattering [1], in general a few percent, strongly disagree with numerical simulations which predict much higher levels. It is supposed that some nonlinear mechanisms are at play which limit the backscattering and which are not properly taken into account in numerical simulations. The present work emphasizes the importance of nonlinear kinetic effects.

In the following we present a new kinetic scenario for SBBS saturation in the high-intensity regime, which can be considered as the final state of strong ion-acoustic  $X$ -type wave-breaking and defect formation [2]. Periodic generation of IAW packets with phase jumps (defects) in between has been observed before in fluid [3] and Korteweg–de Vries (KdV) simulations [4,5]. These calculations indicate the importance of deviation from quasineutrality. However, fluid simulations disregard kinetic effects and KdV simulations are restricted to the weakly nonlinear regime. Some hybrid calculations are available which allow for ion resonant effects and ion trapping [6]. Although they present simulations of long duration and large plasmas, they neglect possible electron kinetic effects by assuming an isothermal Boltzmann response for the electrons. Recent full particle-in-cell (PIC) simulations [7] were limited insofar as they used a driver. Nevertheless, they showed the importance of electron kinetic effects already at much lower intensities.

We present full PIC calculations in a regime of realistic parameters for the duration of the simulation, of the plasma length, and for high intensities. In particular, the duration of the simulation is important as the first cavity appears after only a few ion-acoustic periods. The calculations were performed for a one-dimensional (1D) configuration

(1D in space and 2D in velocity space) using the fully relativistic code EUTERPE [8].

The computational setup for the PIC simulations was as follows. A plasma density above the quarter-critical density of  $n_e = 0.3n_c$  was used in order to avoid excitation of Raman backscattering. The temperature ratio was set to  $ZT_e/T_i = 50$  with  $Z = 1$  and  $T_e = 500$  eV. This corresponds to negligible ion Landau damping. The characteristic sound velocity for the initially thermal plasma was  $c_s/c_0 = 0.7 \times 10^{-3}$ , with  $c_0$  the vacuum speed of light. The SBBS driven IAW period was  $\tau_{cs} = 2.4$  ps. The ratio of the electron quiver velocity,  $v_{osc} = eE/m_e\omega_0$ , to the speed of light is constant in time, with a value of  $v_{osc}/c_0 = 0.085$ . This corresponds to an intensity of  $I = 1 \times 10^{16}$  W/cm<sup>2</sup> for a laser wavelength of  $\lambda_0 = 1$   $\mu$ m. We also used a realistic mass ratio of ions to electrons,  $m_i/m_e = 1836$ . The plasma was composed of two ramps ( $1\lambda_0$  each) and a plateau of a length of  $38\lambda_0$ . The plasma was separated from the boundaries by large vacuum regions ( $40\lambda_0$  each) such that the boundary conditions for the particles do not influence the interaction physics for the duration of the simulation. The simulation time was  $(2.5 \times 10^4)\omega_0^{-1}$  which corresponds to 12.5 ps for  $\lambda_0 = 1$   $\mu$ m. The time step has been set to  $\Delta t = (5 \times 10^{-2})\omega_0^{-1}$  with  $\omega_0 = k_0c_0$  being the frequency of the laser light. The plasma was represented by  $4 \times 10^5$  particles distributed over 5200 cells of width  $\Delta x \approx (0.8 \times 10^{-2})\lambda_0 \approx 0.85\lambda_D$ , with  $\lambda_D = (T_e/4\pi n_e e^2)^{1/2}$  being the Debye length of the initial thermal plasma. The calculations take place in the strong coupling limit [9] as  $4k_0c_s\omega_0/\omega_{pe}^2 \approx 0.01 \ll (v_{osc}/v_e)^2 = 7.2$ , with  $v_e = \sqrt{T_e/m_e}$  the thermal velocity.  $\omega_{pe} = (4\pi n_e e^2/m_e)^{1/2}$  is the electron plasma frequency.

The time evolution of the density profile (Fig. 1) shows the appearance of density cavities after several picoseconds into the interaction process. The cavity formation is the final state of the steepening of a driven IAW packet. The continued driving by the incident electromagnetic wave induces a three-step transition from (i) an originally nonlinear hydrodynamic regime (harmonics and steep-

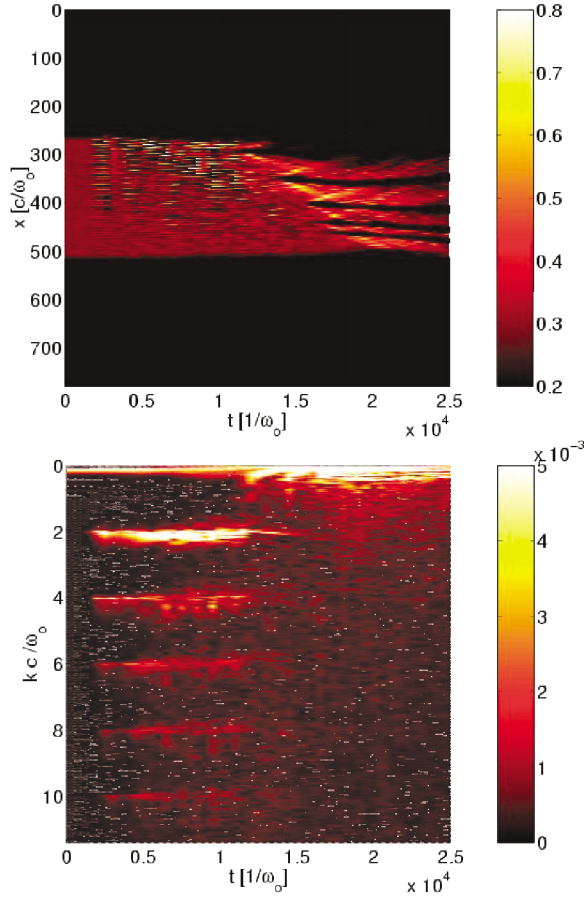


FIG. 1 (color). Time evolution of the density. Top: The ion density in real space; the color bar gives the density in units of the critical density. Bottom: The corresponding Fourier transform.

ening) via (ii) a mixed hydrokinetic regime (large population of trapped ions and X-type wave breaking) to (iii) a purely kinetic regime beyond the wave-breaking limit (ion and electron heating and the disappearance of the resonance IAW).

The initial process can be well described by simplified analytical models [4], but they cannot account for wave breaking and its consequences. This X-type wave breaking has been observed before [2] in full PIC simulations, but its final state has not been considered. According to the KdV simulations and hydrosolutions [4,5], the nonlinear state of the driven IAW consists of a shallow density depression followed by a number of narrow high-density peaks. The continued steepening of the wave-packet solution leads to a point where the compressed ion density peak is no longer subject to quasineutrality. The local ion distribution can be approximated by a  $\delta$ -function-like structure of a thickness comparable to the Debye length. The electrons, because of their much larger thermal velocity, escape the compressed region and are much more spread out, forming a Lorentzian-like distribution. Consequently, the ion charge is not balanced and a Coulomb-like explosion on the scale of the Debye length terminates the ion peaks. This is the

X-type wave breaking observed in [2], which gives an acceleration of ions in both directions with velocities up to  $10c_s$ . The first crash is followed by several other collapses of neighboring peaks. The process leading to X-type IAW breaking repeats itself several times. It is a precursor to the subsequent nonlinear evolution which induces strong electron heating. This heating allows for a second kind of Coulomb explosion to take place, albeit on a much larger scale ( $\sim 2\lambda_0$ ) and at lower density  $n/n_c$  which is responsible for the cavity formation. As the spatial extension of a wave packet is of the order of  $\lambda_{cs} = \lambda_0/2$ , about four IAWs participate in the formation of such a cavity. The process of cavity formation repeats itself several times, and the final state is a sequence of cavities.

The cavities enclose trapped electromagnetic fields (Fig. 2), which seem to correspond to electromagnetic solitons which have been observed before in underdense plasmas interacting with strong laser fields, albeit for different parameter regimes than the present simulations [10,11]. Each cavity is surrounded by high-density shoulders which are due to compression and shock formation as the cavity is created. Inside the cavities the electromagnetic field energy is enhanced by about a factor of 30 due to a resonatorlike effect. The enhancement factor requires a reflectivity of the order of 97% on the cavity walls. As the cavity is almost void of plasma, the reflectivity is given by the Fresnel formula  $r = [(N - 1)/(N + 1)]^2$  with the refractive index of the surrounding plasma being  $N = \sqrt{1 - n_e/n_c}$ . Such a strong enhancement of the electromagnetic field requires a surrounding density at least of the order of the critical density  $n_c$ . The electromagnetic pressure inside the cavities is balanced by the surrounding plasma pressure. Initially, the thermal plasma energy is almost equal to the electromagnetic energy. The increase  $E^2/E_0^2 \approx 30$  in the transverse electromagnetic field energy is balanced by an increase of the density with respect to the

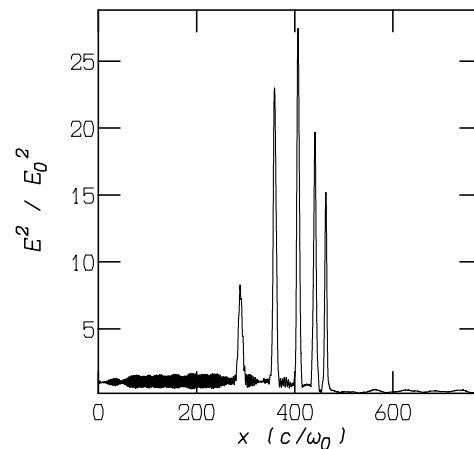


FIG. 2. Transverse electric field energy at  $t = (1.8 \times 10^4)\omega_0^{-1}$  after all cavities have been established. Note that even after a time interval  $\Delta t = (7 \times 10^3)\omega_0^{-1}$  the positions and amplitudes of the electromagnetic solitons have changed very little. The magnetic field energy displays a similar behavior.

initial value by a factor of 5–6 and by an increase of the bulk electron temperature by a similar factor. This increase in electron bulk temperature is due to strong absorption which appears with the formation of the first cavity. Fast electrons of energies up to 40 keV are created during cavity formation. Their origin is the ponderomotive force due to the strong variation of the electromagnetic field inside the cavity. One has initially  $E_0^2/4\pi n_e T_e \sim 2$ . The energy of the accelerated electrons should be of the order of the ponderomotive potential,  $m_e v_h^2 \approx e\Phi_{\text{pond}}$ . One therefore has  $m_e v_h^2 \sim E^2/4\pi n_e \approx T_e(E_0^2/4\pi n_e T_e)(E^2/E_0^2) \times (n_e/n_c) \approx 20T_e$ , which gives the right order of magnitude.

The formation of cavities induces strong changes in the reflectivity. The time evolution of the backscattered intensity, Fig. 3, shows three distinct time intervals of different reflectivity levels (corresponding to the three regimes of the density evolution mentioned above). The first interval of a high reflectivity of the order of 90% and of moderate oscillations extends to  $t = (6 \times 10^3)\omega_0^{-1}$ . During this time, the IAW grows, generates its harmonics, and traps the ions. In the second phase, up to  $t = (1.5 \times 10^4)\omega_0^{-1}$ , characterized by large oscillations in the reflectivity and the density, the IAW packets crash and the first cavities appear. The time delay between a crash and the formation of a cavity is of the order of a few hundred  $\omega_0^{-1}$ . Each time a wave packet crashes, a large peak in the reflectivity appears. With each cavity formed, the average value of the reflectivity decreases, because the plasma length available for SBBS amplification has diminished. The third phase corresponds to a saturated reflectivity at a level of about 5%. Several factors contribute to the final low-level saturation and the inhibition of new SBBS buildup: (i) the effective gain length is reduced due to the presence of the cavities; (ii) the gain is affected by the strong heating of the electrons as the growth rate depends on the ratio  $v_{\text{osc}}/v_e$ ; (iii) a state of low- $k$  broadband fluctuations (Fig. 4) which have a short correlation length and therefore a small SBBS gain; and (iv) finally, a very inhomogeneous phase space

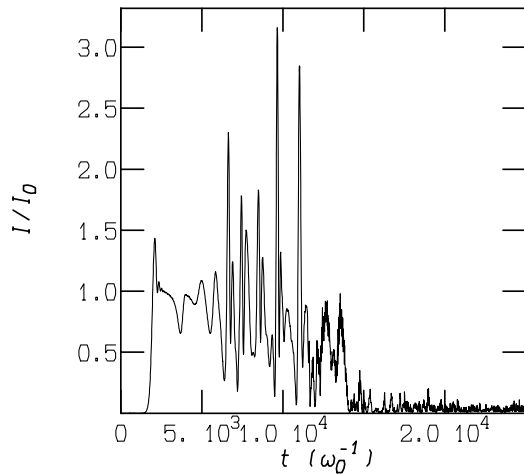


FIG. 3. Temporal variation of the backscattered intensity with respect to the incident intensity.

for the ions which implies the presence of detuning effects [6] for the plasma between the cavities.

The time evolution of density and backscattered radiation reflects itself in the IAW spectrum (Fig. 1, bottom panel). A broadened IAW fundamental appears once the initial exponential growth of the reflectivity is over [at  $t = (2 \times 10^3)\omega_0^{-1}$ ], which is half an IAW period for our parameters. IAW harmonics (up to four in Fig. 1) appear when the fluctuation level  $\delta n/n_e$  is of the order of  $(k_{cs}\lambda_D)^2 \sim 0.01$ , i.e., soon afterwards. Their amplitudes are comparable, which is a signature of a strongly nonlinear IAW. The presence of the harmonics does not imply a low saturated regime of reflectivity (see Fig. 3). We identify a characteristic pulsation of period  $\sim 1500\omega_0^{-1}$  for the sidebands. The average amplitudes of the harmonics remain constant until the first cavity is formed [at  $t = (1.2 \times 10^3)\omega_0^{-1}$ ]. This terminates the IAW harmonics, reduces the average value of the reflectivity to about 50%, and makes the broadening of the fundamental disappear. With the formation of the subsequent cavities, the fundamental of the resonant IAW itself disappears [ $t = (1.5 \times 10^4)\omega_0^{-1}$ ] and the reflectivity enters a saturated, quasi-stationary kinetic regime. In the Fourier spectrum, Fig. 4, the cavity formation manifests itself in regular structures ( $\sim 0.2k_0$ ), which are complemented by a broadband spectrum. The moment of cavity formation is also correlated with the onset of strong energy absorption by electrons and ions. Near the end of the calculation, after all cavities have been formed, reflectivity is at  $\sim 5\%$  transmission at  $\sim 20\%$  and  $\sim 75\%$  of the laser energy is absorbed. The absorbed energy goes in roughly equal amounts to electrons and ions

Figure 5 represents the dispersion diagram of the IAW. One clearly discerns two branches of the dispersion relation corresponding to the forward (positive  $\omega/\omega_{cs}$ ) and backward (negative  $\omega/\omega_{cs}$ ) propagating IAWs. Calculations at lower intensity ( $I = 1 \times 10^{15}$  W/cm<sup>2</sup> at  $\lambda_0 = 1 \mu\text{m}$ ) show only the branch corresponding to an IAW propagating in the forward direction. The branch

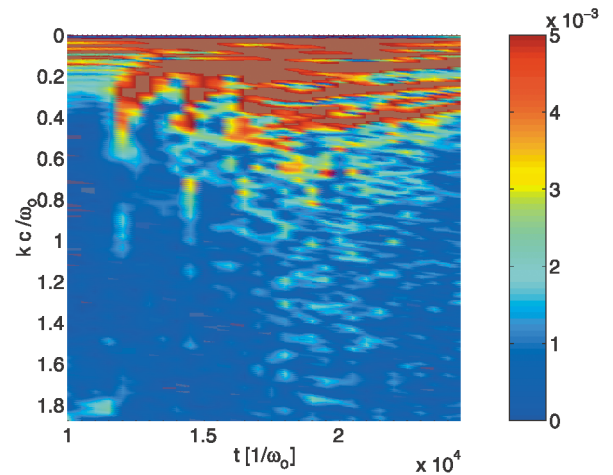


FIG. 4 (color). Fourier spectrum of the density between  $k \approx 0$  and the original position of the IAW fundamental.

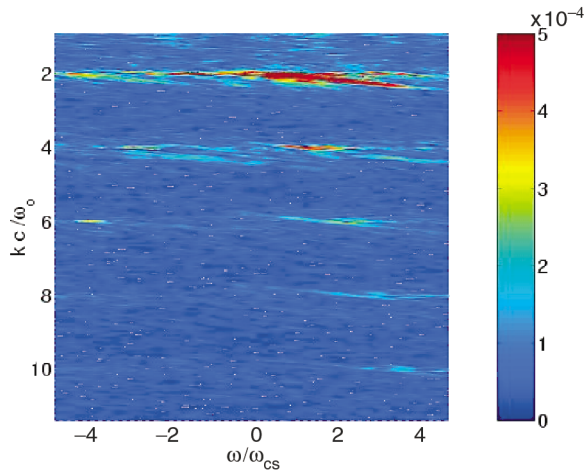


FIG. 5 (color). Dispersion diagram showing the fundamental and the first four harmonics of the IAW.

relating to the backward traveling IAW is due to Brillouin backscatter of the reflected wave itself [12]. This mechanism manifests itself only at sufficiently high intensity. The fundamental and the first harmonic show a very large spectral broadening, which is due to two effects: (i) in a strongly driven regime the IAW dispersion relation is modified and the wave becomes a quasimode of frequency  $\omega = \frac{1-i\sqrt{3}}{2}(k_0^2 v_{\text{osc}}^2 \omega_{pi}^2 / \omega_0)^{1/3}$  [9], giving a broadening factor of  $\sim 2$  for the dominant part of the spectrum; (ii) the variations of the IAW amplitude on the time scale of a fraction of the fundamental IAW period, associated with the pulsations of the reflectivity coefficient in the time interval  $[(6-12) \times 10^3] \omega_0^{-1}$  (Fig. 3). The higher harmonics show more narrow spectra, which are more in agreement with the linear dispersion relation.

This kinetic saturation mechanism was observed in the intensity range from  $5 \times 10^{15}$  to  $1 \times 10^{16}$  W/cm<sup>2</sup> at  $\lambda_0 = 1 \mu\text{m}$ . Assuming intensity fluctuations of the order of 10 in the randomized laser beam, one may expect this mechanism to operate for average intensities of the order of  $10^{15}$  W/cm<sup>2</sup>. Lowering the intensity delays the onset of cavity formation as the gain factors are smaller, and consequently the X-type wave breaking and the onset of the strongly kinetic regime is delayed. The cavitation process is associated with strong electron kinetic effects, and we therefore postulate that it is not observable with hybrid models which assume a fixed electron temperature. Significant electron acceleration and heating are the new elements in this SBBS saturation scenario. Performing the same calculations for  $ZT_e/T_i = 5$  and 10 (using the same electron temperature of 500 eV), while keeping all remaining parameters fixed, shows exactly the same scenario and the same low-level saturated state for the reflectivity. It is only the time scale for the onset of cavitation and the distribution or number of cavities formed that change.

This indicates that linear Landau damping hardly plays a role in the high-intensity regime. Simulations for an electron temperature of 3 keV and the same temperature ratio of 50 reproduce the scenario of cavitation and saturation. As the size of the cavities ( $\sim 2\lambda_0$ ) is small with respect to characteristic longitudinal scale length and to the transverse dimension of a laser beam ( $20\lambda_0-30\lambda_0$ ), we expect the mechanism to reproduce itself in higher dimensions with similar effects.

In summary, we have shown that the formation of cavities, which disrupt internally the homogeneous plasma, can account for the saturation of SBBS at levels of a few percent. The temporal evolution of the reflectivity from a large average value with small oscillations via a phase of large average value and strong oscillations to a saturated regime corresponds to the transition of the plasma dynamics from a regime dominated by hydrodynamic nonlinearities via a regime of X-type wave breaking to a final purely kinetic regime. The calculations also show that neither the generation of higher harmonics nor the presence of strong ion trapping is sufficient to induce a low saturation of the average reflectivity level. The mechanism might also be at play at much lower intensities provided other saturation mechanisms do not operate on a shorter time scale. As the plasma is an easily deformable medium, the SBBS buildup in the high-intensity regime will always lead to cavity formation, if the gain is large enough; i.e., backscattering in plasmas contains its own self-limiting procedure. This is in contrast to solids or fibers where SBBS will always attain 100% if the medium is long enough.

The calculations were performed at the Bordeaux University computing center M3PEC and at the *Centre de Calcul Recherche et Technologie (CCRT)* of the CEA.

- 
- [1] C. Labaune *et al.*, Plasma Phys. Controlled Fusion **46**, B301 (2004).
  - [2] D.W. Forslund *et al.*, Phys. Fluids **18**, 1017 (1975).
  - [3] D. Pesme *et al.*, Plasma Phys. Controlled Fusion **44**, B53 (2002).
  - [4] J. Candy, W. Rozmus, and V.T. Tikhonchuk, Phys. Rev. Lett. **65**, 1889 (1990).
  - [5] W. Rozmus *et al.*, Phys. Fluids B **4**, 576 (1992).
  - [6] L. Divol *et al.*, Phys. Plasmas **10**, 3728 (2003).
  - [7] C. Riconda *et al.*, “Electron Kinetic Effects in the Nonlinear Evolution of a Driven Ion-Acoustic Wave” (to be published).
  - [8] G. Bonnaud and G. Reisse, Nucl. Fusion **26**, 633 (1986).
  - [9] D.W. Forslund *et al.*, Phys. Fluids **18**, 1002 (1975).
  - [10] S. Bulanov *et al.*, Phys. Fluids B **4**, 1935 (1992); Phys. Rev. Lett. **82**, 3440 (1999).
  - [11] A.B. Langdon and B.F. Lasinski, Phys. Fluids **26**, 582 (1982).
  - [12] T. Speziale *et al.*, Phys. Fluids **23**, 1275 (1980); A. Langdon and D. Hinkel, Phys. Rev. Lett. **89**, 015003 (2002).